Multiscale Morphological Segmentation of Gray-Scale Images

Susanta Mukhopadhyay and Bhabatosh Chanda, *Fellow, IEEE*

***Abstract*—In this paper, the authors have proposed a method of segmenting gray level images using multiscale morphology. The approach resembles watershed algorithm in the sense that the dark (respectively bright) features which are basically canyons (respectively mountains) on the surface topography of the gray level image are gradually filled (respectively clipped) using multiscale morphological closing (respectively opening) by reconstruction with isotropic structuring element. The algorithm detects valid segments at each scale using three criteria namely growing, merging and saturation. Segments extracted at various scales are integrated in the final result. The algorithm is composed of two passes preceded by a preprocessing step for simplifying small scale details of the image that might cause over-segmentation. In the first pass feature images at various scales are extracted and kept in respective level of morphological towers. In the second pass, potential features contributing to the formation of segments at various scales are detected. Finally the algorithm traces the contours of all such contributing features at various scales. The scheme after its implementation is executed on a set of test images (synthetic as well as real) and the results are compared with those of few other standard methods. A quantitative measure of performance is also formulated for comparing the methods.**

***Index Terms*—Closing by reconstruction, gray-level image segmentation, morphological towers, multiscale morphology, opening by reconstruction, performance analysis.**

I. Introduction

SEGMENTATION is a very commonly used and important step in image analysis and computer vision. The purpose of image segmentation is to decompose an image domain into a number of disjoint regions so that the features within each region have visual similarity, strong statistical correlation and reasonably good homogeneity. Image segmentation techniques may be classified into a number of groups depending on the approach of the concerned algorithm. These include *feature thresholding, contour based techniques, region based techniques, clustering, template matching* [1], etc. Each of these approaches has its own merits and demerits in terms of applicability, suitability, performance, computational cost etc. and no one can meet all the demands. A gradient thresholding technique, for example, suffers from the problem of yielding contours with nonuniform thickness as well as discontinuities due to difficulty in selecting optimum threshold. The well-known watershed algorithm—a morphological instance of region based approach, apart from being computationally intensive, suffers from over or under-segmentation due to improper choice of marker points.

Segmentation of gray level images is a well studied problem. There exist several methods for segmenting gray-level images [2], [3], [4]. Gray-level thresholding is one of the oldest techniques for image segmentation [3]. Threshold may be chosen based on *histogram* [6] or on gray-level co-occurrence matrix [5], or by analyzing intra-region and inter-region homogeneity [7]. Canny [8] has suggested a contour based technique employing hysteresis thresholding. Anisotropic diffusion and PDE-based regularization for segmentation has been developed by Romeny [9], Weickert [10]. Segmentation algorithms based on nonlinear diffusion have been devised by Niessen *et al.* [11], Jackway [12]. A different approach based on local monotonicity has been suggested by Acton *et al.* [13]. Another segmentation method proposed by Frank *et al.* [14], uses combination of optimal and adaptive thresholding. An overview of border detection and edge linking methods in connection to segmentation can be found in [15]. Region-based segmentation techniques, by and large, detect homogeneity in terms of parameters like gray-level, color, texture etc. A number of region growing techniques for color image segmentation may be found in [16], [17], [18]. A hierarchical merging method has been suggested by Goldberg *et al.* [19]. The watershed algorithm and its variants [20], [21], [22], are found to produce reasonably good segmentation results. In a different approach Malik *et al.* [23] have suggested a graph partitioning method for segmenting gray-level images. Manjunath *et al.* [24] in another approach have devised a technique for image segmentation based on edge flow. An unsupervised multiresolution scheme for segmenting images with low depth is proposed by Wang and *et al.* [25]. Image segmentation using neuro-fuzzy techniques, genetic algorithms, wavelets, fractals etc. may be found in [26], [27], [28], [29]. Acharya *et al.* [30] have made a very good review of biomedical image segmentation techniques.

Mathematical morphology is a well-known technique used in image processing and computer vision [31], [32], [41]. This set theoretic, shape oriented approach treats the image as a set and the kernel of operation, commonly known as *structuring element* (SE), as another set. Different standard morphological operations namely *dilation, erosion, opening, closing* etc. are basically set-theoretic operations between these two sets. The shape and the size of the SE play important role in detecting or extracting features of given shape and size from the image. Application of mathematical morphology in gray-level image segmentation can be found in [12], [33], [34]. If the set representing the SE is convex then dilation of the SE with itself $(n-1)$

times produces the nth homothetic of the SE keeping its shape intact. Morphological operations with such scalable SE's may be used in multiscale image processing. The work presented in this paper is an example of this approach.

Dealing with the objects of different size and shape in the image is a very interesting aspect of machine vision. In most of the image processing operators, the concept of scale of the objects is not incorporated explicitly. In general, an image comprises of objects or features of different scales. On the other hand, most spatial domain image processing techniques use the notion of *local neighborhood* which does not take care of the scale of the object contained in that neighborhood. As a result, the operator processes objects of various scales with equal emphasis. The objects in an image should be processed as per their scales. Thus the need for processing the image based on the size or scale has initiated several *multiscale* and *multi resolution* techniques. Multiscale and multi resolution techniques extract scale specific information from the image and integrate them to produce desired output. The entire process may be linear or nonlinear and accordingly it gives rise to a linear or nonlinear scale space representation of the image under study. A lot of literatures [35], [37], [38], [39], [40] are available describing the properties and issues of scale space.

In this paper we have proposed a method for segmenting gray-level images using multiscale morphology. The paper is organized in the following way. In Section II we have discussed on multiscale morphology, the definition of *morphological tower* and its properties in order to satisfy various requirements of scale space representation. In Section III we have presented the proposed method. The theoretical formulation of the proposed method is discussed elaborately in Section III-A while the implementational details are given in Section III-B. The experimental results are presented in Section IV. Finally, the concluding remarks are given in Section V.

II. Multiscale Mathematical Morphology

Mathematical Morphology is a powerful tool for dealing with various problems in image processing and computer vision. Morphological operations, namely *erosion, dilation, opening, closing, top-hat transformation* etc. are used for extracting, modifying, manipulating the features present in the image based on their shapes. The shape and the size of SE play crucial roles in such type of processing and are therefore chosen according to the need and purpose of the associated application. The *function- and set-processing* (FSP) system [42] is widely used in morphology. FSP dilation and erosion of a gray-level image $g(r, c)$ by a two dimensional point set B are defined respectively as

$$(g \oplus B)(r, c) = \max\{g(r-k, c-l) \,|\, (k, l) \in B\} \quad (1)$$

$$(g \ominus B)(r, c) = \min\{g(r+k, c+l) \,|\, (k, l) \in B\}. \quad (2)$$

Opening (closing) is sequential combination of erosion (dilation) and dilation (erosion). Though the structuring element B takes care of the shape of the features while processing the image, it cannot, however, treat objects of same shape but of different size equally. Thus, for processing objects based on their shape as well as size we incorporate a second attribute to the structuring element which is its *scale*. A structuring element along with its higher order homothetics can process the image features based on shape as well as size. Such types of morphological operations are termed as *multiscale morphology* [32], [42]. Multiscale opening and closing [43] are defined, respectively, as

$$(g \circ nB)(r, c) = ((g \ominus nB) \oplus nB)(r, c) \quad (3)$$

$$(g \bullet nB)(r, c) = ((g \oplus nB) \ominus nB)(r, c) \quad (4)$$

where n is an integer representing the scale factor of the structuring element B. The nth homothetic of a convex SE B is obtained by dilating B recursively $n-1$ times with itself as

$$nB = B \underbrace{\oplus B \oplus B \oplus \cdots \oplus B}_{n-1 \text{ times}}. \quad (5)$$

Conventionally, $nB = \{(0, 0)\}$ when $n = 0$.

Thus, multiscale morphological operations decompose the given image into a set of filtered images. Now in doing so, the system of such operations should satisfy the properties like i) *causality* and ii) *edge localization* [44], [45], [46]. By the term "causality" we mean no regional extrema and, consequently, edge is introduced as the scale increases. The objective is to distribute the given information and not to create new ones. The property "edge localization" demands no drift of edge from its original position. The system is also expected to be *scale-calibrated*, i.e., the filtered image produced by an SE of a particular scale should strictly contain the features of that scale only. Apart from these, the directional or rotational invariance of the associated operation can be achieved using an isotropic SE.

The multiscale opening produces flat regions by removing bright objects or its parts smaller than the SE. The properties: $g \circ B \leq g$ and $g \circ iB \geq g \circ jB$ for $i < j$ imply that no new bright feature (or, in other words, regional maxima) is generated at higher scales due to opening. In case of multiscale closing, no new dark feature (or, in other words, regional minima) is generated at higher scales. Secondly, the SE leaves the features larger than it unaffected. However, removal of parts of an object introduces new edges or causes drifts of the existing edges [Fig. 1]. The main disadvantage of conventional opening and closing is that they do not allow a perfect preservation of the edge information [47]. Bangham *et al.* [46] suggested a scale-space operator, called M- and N-sieves, which satisfies the properties mentioned above. This operator emphasizes only on the size of the features, but ignores their shape completely. However, it is possible to design morphological filters by reconstruction that satisfy these requirements and consider both shape and size of the features. Morphological multiscale opening and closing by reconstruction [34], [48], [49], are two such filters.

The elementary geodesic dilation, denoted by $\delta_X^1(g, \rho)$, of size one (i.e., the smallest size in discrete domain) of the image g with respect to a reference image ρ is defined as the minimum between g dilated by an SE X of size one and ρ. Hence,

$$\delta_X^1(g, \rho) = \min(g \oplus X, \rho). \quad (6)$$

(a) (b) (c)

Fig. 1. (a) Original image, (b) result of conventional opening of (a) using a disk SE, and (c) result of opening by reconstruction of (a) with same SE.

Similarly, the elementary geodesic erosion, denoted by $\epsilon_X^1(g, \rho)$, of size one is defined as the maximum between g eroded by X of size one and a reference image ρ. Hence,

$$\epsilon_X^1(g, \rho) = \max(g \ominus X, \rho). \tag{7}$$

Now geodesic dilation and erosion of arbitrary size are obtained through iteration as

$$\delta_X^i(g, \rho) = \min\left(\delta_X^{(i-1)}(g, \rho) \oplus X, \rho\right) \tag{8}$$

$$\epsilon_X^i(g, \rho) = \max\left(\epsilon_X^{(i-1)}(g, \rho) \ominus X, \rho\right) \tag{9}$$

for $i = 1, 2, 3, \ldots$. Conceptually this may continue indefinitely, but for all practical purposes iteration is terminated at an integer n such that $\delta_X^n(g, \rho) = \delta_X^{(n-1)}(g, \rho)$ and, similarly, when $\epsilon_X^n(g, \rho) = \epsilon_X^{(n-1)}(g, \rho)$; because no change would occur after that. This stable output is termed as *reconstruction by dilation* and is denoted by $\delta^{(rec)}(g, \rho)$, i.e.,

$$\delta^{(rec)}(g, \rho) = \delta_X^n(g, \rho).$$

Similarly we have *reconstruction by erosion* denoted by $\epsilon^{(rec)}(g, \rho)$, i.e.,

$$\epsilon^{(rec)}(g, \rho) = \epsilon_X^n(g, \rho).$$

Based on this operation *opening by reconstruction of opening*, or simply, *opening by reconstruction* denoted by $g \overline{\circ} B$, may be defined as

$$g \overline{\circ} B = \delta^{(rec)}(g \circ B, g). \tag{10}$$

Similarly, *closing by reconstruction* denoted by $g \overline{\bullet} B$ may be defined as

$$g \overline{\bullet} B = \epsilon^{(rec)}(g \bullet B, g). \tag{11}$$

Therefore, morphological opening by reconstruction in its first step eliminates bright features that do not fit within the SE applying simple opening. In its second stage, it dilates iteratively to restore the contours of components that have not been completely removed by opening and a reconstruction is accomplished by these iterative dilations using the original image g as the reference, i.e., choosing $\rho = g$. Similar analysis holds for "closing by reconstruction" in case of dark features. As a result, problems like introduction of new edges and edge drift do not arise in case of opening by reconstruction and closing by reconstruction. Hence, multiscale system designed with these operators satisfy causality and edge localization properties. Fig. 1 illustrates the difference between the conventional opening and the opening with reconstruction with an example image.

When these operators, i.e., open (close) by reconstruction, are used with multiscale SEs, the output image should contain only features of that and higher scales. The difference between the images opened at two successive scales will then contain features of a particular scale only. In essence, in the difference image, the features, which, or, at least a part of which, contains the SE at that scale are present completely and others are removed. Thus, the system can be termed as *scale calibrated*. In the following discussion, unless otherwise mentioned, "open" refers to "open by reconstruction" and "close" refers to "close by reconstruction," and consequently "$\circ$" stands for "$\overline{\circ}$" and "$\bullet$" stands for "$\overline{\bullet}$."

A *morphological tower* is a stack of images containing morphologically filtered images obtained by using a family of SEs comprising of a convex and compact SE and its higher order homothetics. A morphological tower resembles an image pyramid in many aspects. An image pyramid consists of a stack of images with decreasing resolution and size of the image. A morphological tower on the other hand stacks the images filtered at increasing scale leaving the resolution unchanged. Fig. 2 illustrates the structures of an image pyramid and a morphological tower. Thus, a morphological tower corresponding to opening consists of a stack of images opened with a family of SEs. Some applications of morphological tower may be found in [50], [51], [52].

III. Proposed Method

A gray level image typically consists of both bright and dark object features which, in general, have a distribution with respect to size or *scale*. The basic objective of a segmentation algorithm is to isolate or sketch out the most optimal contours of these bright and dark features. Though the proposed method is basically region based, it produces contours enclosing pixels that have properties distinguishable from their immediate neighborhoods. In this section we first present the theoretical background of the proposed method and then the implementational details.

A. Theoretical Formulation

A digital gray-tone image is may be viewed as an intensity surface defined over a spatial coordinate system. If $L = \{0, 1, \ldots, L_m\}$ be the set of intensity values and $S = \{(x, y): x, y \in Z, 0 \le x \le N_r - 1, 0 \le y \le N_c - 1\}$

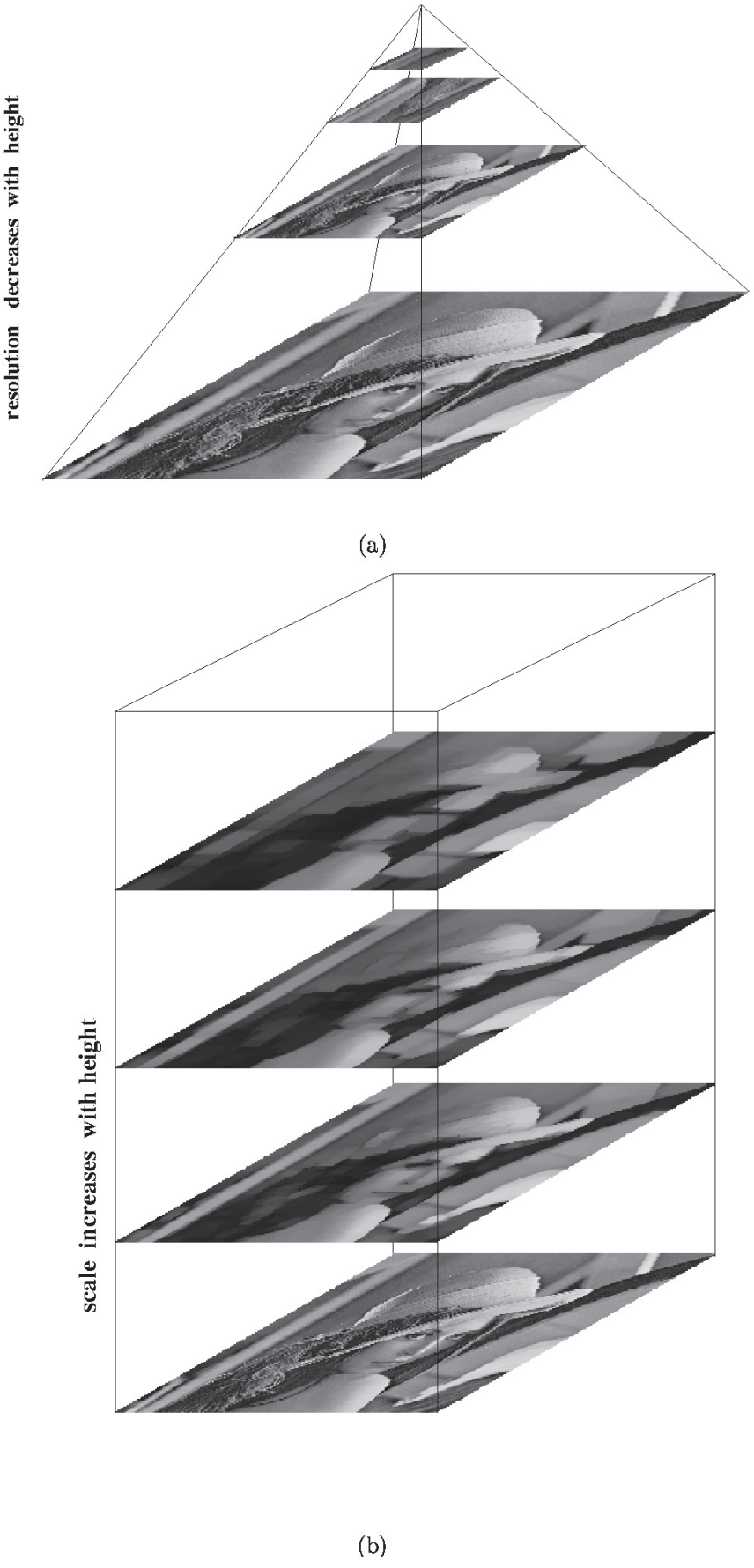

Fig. 2. (a) Image pyramid and (b) morphological tower corresponding to multiscale opening.

be the spatial coordinates of the pixels of the image, the digital image represented as a function g is then defined as

$$g: S \rightarrow L. \tag{12}$$

Thus $g(x, y)$ represents the intensity value of the pixel located at $(x, y) \in S$ and the size of the image is $N_r \times N_c$.

The section of the image at a threshold $k \in L$ is a point set $X^k(g)$ defined as

$$X^k(g) = \{(x, y): (x, y) \in S \text{ and } g(x, y) \geq k, k \in L\}. \tag{13}$$

A binary or black-and-white image g_{bin}: $S \rightarrow \{0, 1\}$ constructed from this point set $X^k(g)$ as

$$g_{bin}(x, y) = \begin{cases} 1, & \text{if } (x, y) \in X^k(g) \\ 0, & \text{otherwise.} \end{cases}$$

In the proposed formulation we have used multiscale bright and dark top-hat transformation to extract scale specific bright and dark features. A thorough analysis of these extracted features might be necessary for segmentation. The bright top-hat image obtained by filtering by an SE of size i contains all bright features smaller than i as

$$g_i^{top}(x, y) = g(x, y) - (g \circ iB)(x, y). \tag{14}$$

Similarly a dark top-hat or a *bottom-hat* transformation at scale i sieves out the dark features smaller than i as

$$g_i^{bot}(x, y) = (g \bullet iB)(x, y) - g(x, y). \tag{15}$$

Now, using (13), the section of the bright and dark top-hat images at a threshold t are given by

$$\Pi_i^t = X^t[g_i^{top}] = \{(x, y) \in S: g_i^{top}(x, y) \geq t, t \in L\} \tag{16}$$

$$\Upsilon_i^t = X^t[g_i^{bot}] = \{(x, y) \in S: g_i^{bot}(x, y) \geq t, t \in L\}. \tag{17}$$

The point sets Π_i^t and Υ_i^t basically contain the coordinates of the supports of the features at scale i that are present in the bright and dark top-hat images respectively. Now, if the value of the intensity threshold t is kept fixed through out the process, the superscript t may be dropped out from the notations of the point sets. In such a case we may simply use Π_i and Υ_i, respectively.

Since both the bright and dark top-hat transformation are *extensive* [41], we necessarily have

$$\Pi_0 \subset \Pi_1 \subset \cdots \subset \Pi_i \subset \Pi_{i+1} \subset \cdots \subset \Pi_N \tag{18}$$

$$\Upsilon_0 \subset \Upsilon_1 \subset \cdots \subset \Upsilon_i \subset \Upsilon_{i+1} \subset \cdots \subset \Upsilon_N \tag{19}$$

where N is an integer representing the largest scale of objects or features present in the image and it may be same as the size of the image itself. However, in practice, N is much less than the size of the image.

Now, the surface topography of a gray-level image, in general, consists of peaks, valleys and possibly plateaus of different height, width, extent. Consequently, each of the point set Π_i and Υ_i is found to consist of a number of maximally connected subsets [3], so that, each of them can be expressed as

$$\Pi_i = \Pi_i^1 \cup \Pi_i^2 \cup \Pi_i^3 \cup \cdots \cup \Pi_i^p \tag{20}$$

$$\Upsilon_i = \Upsilon_i^1 \cup \Upsilon_i^2 \cup \Upsilon_i^3 \cup \cdots \cup \Upsilon_i^q \tag{21}$$

where p and q are the number of maximally connected subsets in Π_i and Υ_i respectively. In addition, for any pair of distinct subsets of Π_i and Υ_i we strictly have

$$\Pi_i^u \cap \Pi_i^v = \emptyset \tag{22}$$

$$\Upsilon_i^u \cap \Upsilon_i^v = \emptyset \tag{23}$$

for $u \neq v$. The subset Π_i^u (Υ_i^u) basically represents a bright (dark) feature or its part at scale i. In other words, the binary images constructed using these point sets are found to contain a number of isolated black blobs against a white background.

Let us consider two point sets Π_i and Π_{i+1} corresponding to two bright top-hat images at two successive scales i and $(i+1)$. For each subset Π_i^u of Π_i there exists one and only one subset Π_{i+1}^v of Π_{i+1} such that $\Pi_i^u \subseteq \Pi_{i+1}^v$. Let us call such subsets as *corresponding subsets*. It is important to note that the total number of subsets in Π_i and Π_{i+1} may not necessarily be the same. The above statements hold good for point sets Υ_i and Υ_{i+1} also. At any given scale, the subsets Π_i^us of Π_i may encounter one of the following three situations

1) *Growing*: A subset Π_i^u is said to be *growing* if it is a proper subset of its corresponding subset Π_{i+1}^v, i.e., $\Pi_i^u \subset \Pi_{i+1}^v$. In such cases, the black blob represented by the subset Π_i^u in the binary image constructed from Π_i represents the support of a part of a potential feature or object. Fig. 3 illustrates the situation indicating a pair of corresponding subsets at two successive scales. The subset Π_i^1 in the point set Π_i is a proper subset of Π_{i+1}^1 in Π_{i+1}. The dotted contour in Π_{i+1}^1 the growth of Π_i^1 with the scale parameter.
2) *Saturation*: A subset Π_i^u is said to be *saturated* if it is congruent with its corresponding subset Π_{i+1}^v, i.e., $\Pi_i^u = \Pi_{i+1}^v$. In such cases, the black blob represented by the subset Π_i^u covers the support of a feature or object as a whole. This case, as earlier, is illustrated in Fig. 3. The subsets Π_i^2 and Π_{i+1}^2 are congruent.
3) *Merging*: If at least two subsets Π_i^u and Π_i^w have the same corresponding subset Π_{i+1}^v, i.e., $\Pi_i^u \bigcup \Pi_i^w \subseteq \Pi_{i+1}^v$, the constituent subsets Π_i^u and Π_i^w are said to *merge*. Two or more merging subsets might enjoy a subsequent growth or saturation with respect to the scale factor. In such a case, each of them individually represents a complete subfeature which is a distinct part of a large valid feature or object at subsequent higher scale. This situation too, is clarified in Fig. 3. The dark blobs represented by Π_i^3 and Π_i^4 are found to have the same corresponding subset Π_{i+1}^3. These two dark blobs merge into a single larger blob represented by Π_{i+1}^3.

The above observations hold good for Υ_i and Υ_{i+1} also. The proposed algorithm treats the subsets of all three categories at various scales. Accordingly, it constructs the following four point sets, corresponding to both bright and dark features

$$Sat_i^{top} = [\{\Pi_i^u\}: \text{if there exist } u \text{ and } w, \text{ such that, } \Pi_i^u = \Pi_{i+1}^w]$$

$$Sat_i^{bot} = [\{\Upsilon_i^u\}: \text{if there exist } u \text{ and } w, \text{ such that, } \Upsilon_i^u = \Upsilon_{i+1}^w]$$

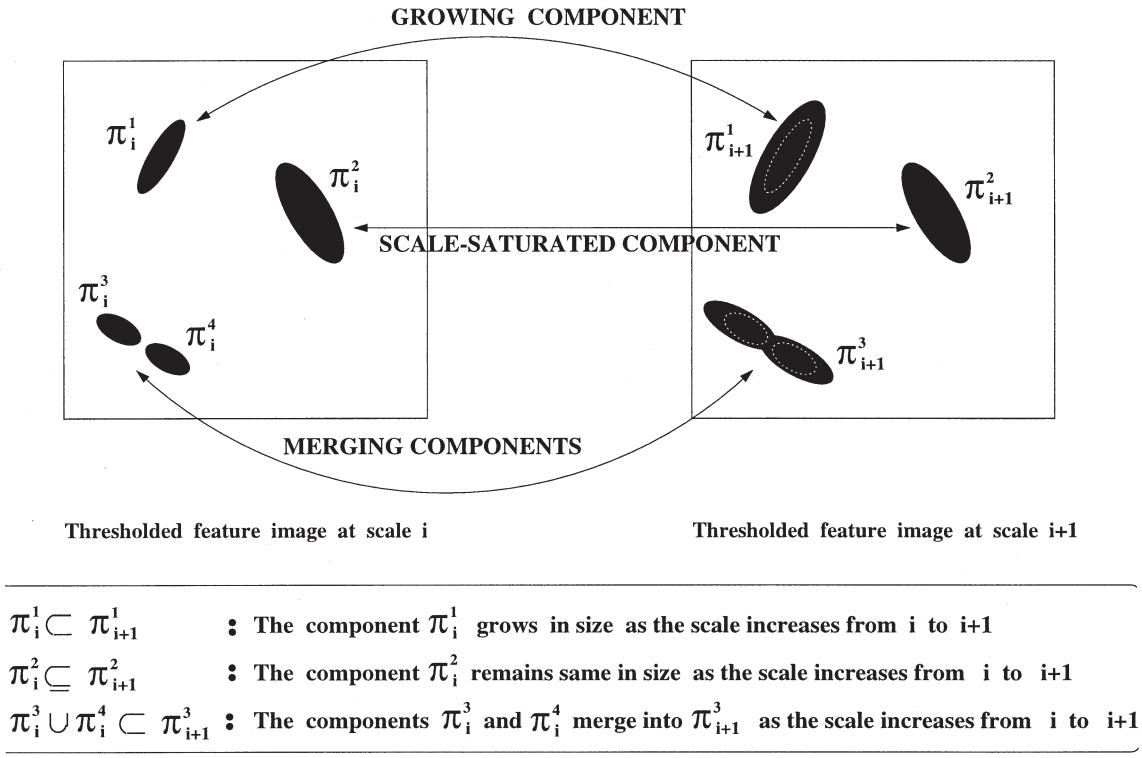

Fig. 3. Different types of similar components at two successive scale i and $i+1$.

$$Mrg_i^{top} = [\{\Pi_i^u \cup \Pi_i^v\} : \text{if there exist } u, v \text{ and } w, \text{ such that, } (\Pi_i^u \cup \Pi_i^v) \subset \Pi_{i+1}^w]$$

$$Mrg_i^{bot} = [\{\Upsilon_i^u \cup \Upsilon_i^v\} : \text{if there exist } u, v \text{ and } w, \text{ such that, } (\Upsilon_i^u \cup \Upsilon_i^v) \subset \Upsilon_{i+1}^w]$$

for $1 \leq i \leq N-1$.

Let $g_i^{top\_bin}$ and $g_i^{bot\_bin}$ be the binary images constructed from the point sets C_i^{top} and C_i^{bot}, respectively, where

$$C_i^{top} = Sat_i^{top} \cup Mrg_i^{top} \tag{24}$$

$$C_i^{bot} = Sat_i^{bot} \cup Mrg_i^{bot}. \tag{25}$$

These binary images comprise of black blobs representing the supports of potential bright and dark features present in the input image at scale i. These blobs, therefore, correspond to the segments of the image. Suppose $g_i^{top\_cont}$ and $g_i^{bot\_cont}$ denote the images containing the closed edges of the blobs in $g_i^{top\_bin}$ and $g_i^{bot\_bin}$ respectively. Hence, the final contour-image g_{cont} is obtained by unifying the contour images at different scales as described by

$$g_{cont} = \left\{\bigcup_{i=1}^{N} g_i^{top\_cont}\right\} \cup \left\{\bigcup_{i=1}^{N} g_i^{bot\_cont}\right\}. \tag{26}$$

Encroachment Problem: Any segmentation algorithm follows its own predefined strategy. Quite often, the gray-level of the pixel or its gradient plays important role in the construction of the segments. The problem of employing gradient magnitude is its noise sensitivity. The proposed algorithm, however, does not employ the knowledge about gradient magnitude. In the proposed algorithm emphasis has been given on the *scale* of the image features while finding the valid segments of the image. The bright and dark features of identical scale are detected sequentially at the same pass of the algorithm. The image, in general,consists of both the bright and dark features at varying scales. When a bright feature is adjacent to a dark feature, a problem of feature overlapping may occur. The SE has no preferential knowledge about the locations of bright and dark features and their scales. Therefore, if the SE is allowed to open and close the image with no restriction regarding when and where to stop, it will cause an overlapping or *mutual encroachment* in the point sets Π_i and Υ_j for same or different values of i and j (Fig. 4 may be referred for an illustration). In other words, the same spatial domain of the image would be claimed as a support of dark as well as bright features at same or different scales. In the foregoing discussion, no restriction was put to the relationship between Π_i and Υ_j. The binary images constructed using Π_i and Υ_j will therefore give rise to overlapping or encroachment in the segmented contours. To get rid of this encroachment problem the following constraint should be enforced.

$$\Pi_i \cap \Upsilon_j = \emptyset. \tag{27}$$

To satisfy the above constraint or, in other words, to avoid encroachment, equations (14) and (15) may be modified, respectively, as

$$g_i^{top}(x, y) = \tilde{g}_{i-1}(x, y) - (\tilde{g}_{i-1} \circ ifB)(x, y) \tag{28}$$

$$g_i^{bot}(x, y) = (\hat{g}_{i-1} \bullet iB)(x, y) - \hat{g}_{i-1}(x, y) \tag{29}$$

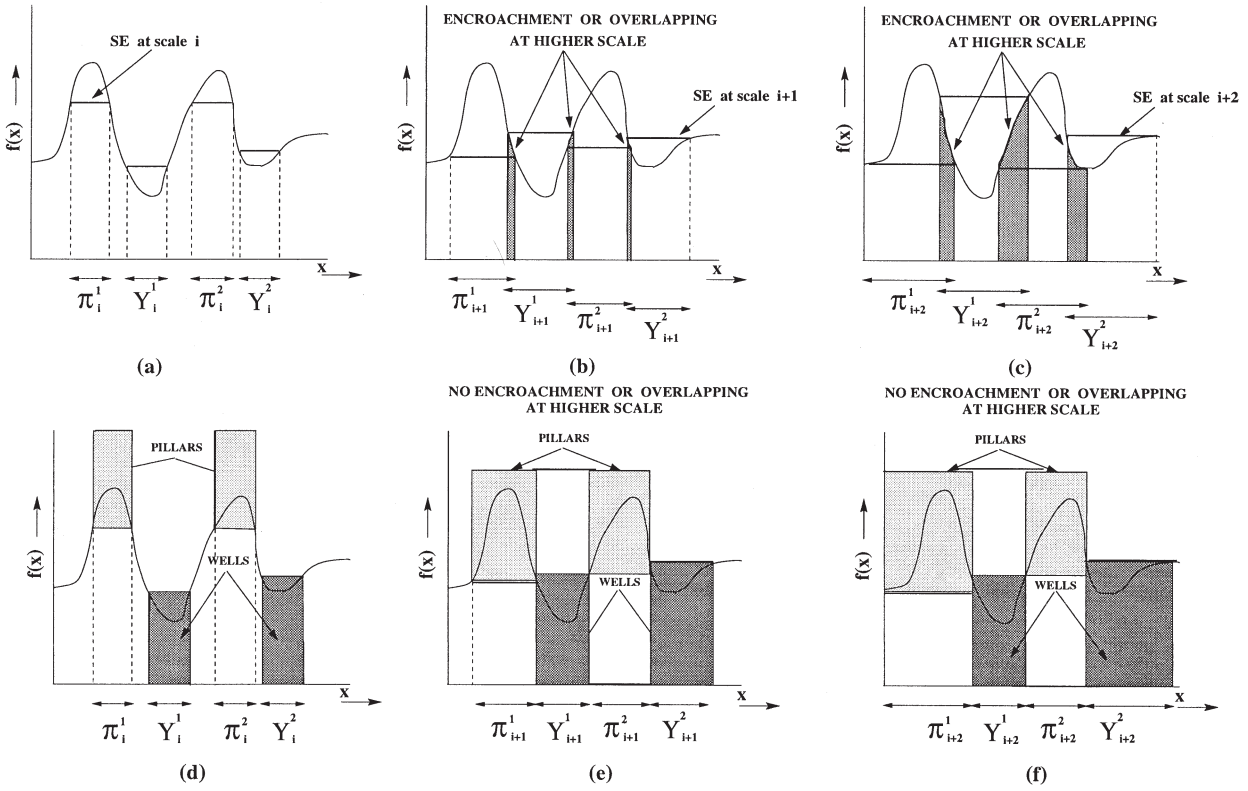

Fig. 4. Illustration of encroachment.

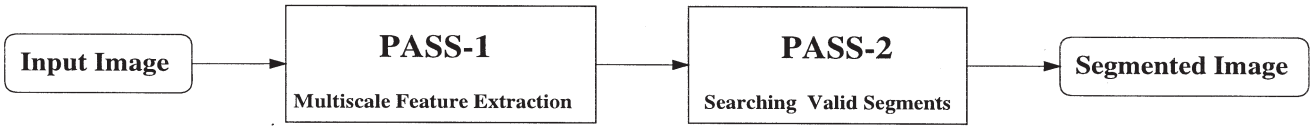

Fig. 5. The stages of proposed multiscale image segmentation algorithm.

where

$$\tilde{g}_i(x, y) = \begin{cases} -\infty, & \text{if } (x, y) \in \Upsilon_{i-1} \\ \tilde{g}_{i-1}(x, y), & \text{otherwise} \end{cases}$$

and

$$\hat{g}_i(x, y) = \begin{cases} \infty, & \text{if } (x, y) \in \Pi_{i-1} \\ \hat{g}_{i-1}(x, y), & \text{otherwise} \end{cases}$$

for $i \geq 1$ and $\tilde{g}_0(x, y) = g(x, y)$ and $\hat{g}_0(x, y) = g(x, y)$. That means once a pixel is marked as a part of a dark feature it is ensured to remain a part of the same dark feature at all higher scales by digging an well of infinite depth at that point. In a similar way, a pixel, once marked as a part of a bright feature at a given scale, is ensured to remain a part of the same bright feature at all higher scales by raising a pillar of infinite altitude at that point. As a result, the possibility of a pixel being detected as a part of a dark as well as a bright feature simultaneously is totally excluded and thus, the encroachment problem is avoided.

B. Implementation

The proposed algorithm starts with a *preprocessing* step as described below. The segmentation scheme is divided into two passes (see Fig. 5) namely i) *multiscale region extraction* and ii) *selection of valid regions that contribute to final segmentation*. Following subsections present them elaborately.

1) Preprocessing: A segmentation algorithm often needs a preprocessing step like noise smoothing to reduce the effect of undesired perturbations which might cause over- and under-segmentation. For example, *Gaussian* filtering is employed in *Marr–Hildreth* [53] and *Canny's* edge detector [8]. The very small scale details (i.e., the sudden discontinuity in gray-value over very small regions) are usually considered as noise. It is a necessity to estimate the scale (or size) of noise particles before removing them. Interested reader may refer to [52] for such analysis. However, the main concern, here, is the segmentation and we have used a morphological method which smooths out noise by applying iterative filtering until the spatial variation of intensity becomes locally monotonic with respect to the SE. The steps of the preprocessing operations are:

1) Perform conventional morphological opening and closing on the input image using an SE of small size. The size of the SE is greater than that of noise particles.
2) Construct the output image by averaging the images resulting after opening and closing.
3) Compare the output image with the input image. If they are identical then halt. Otherwise consider the output image as the input image to the next iteration and go to step 1).

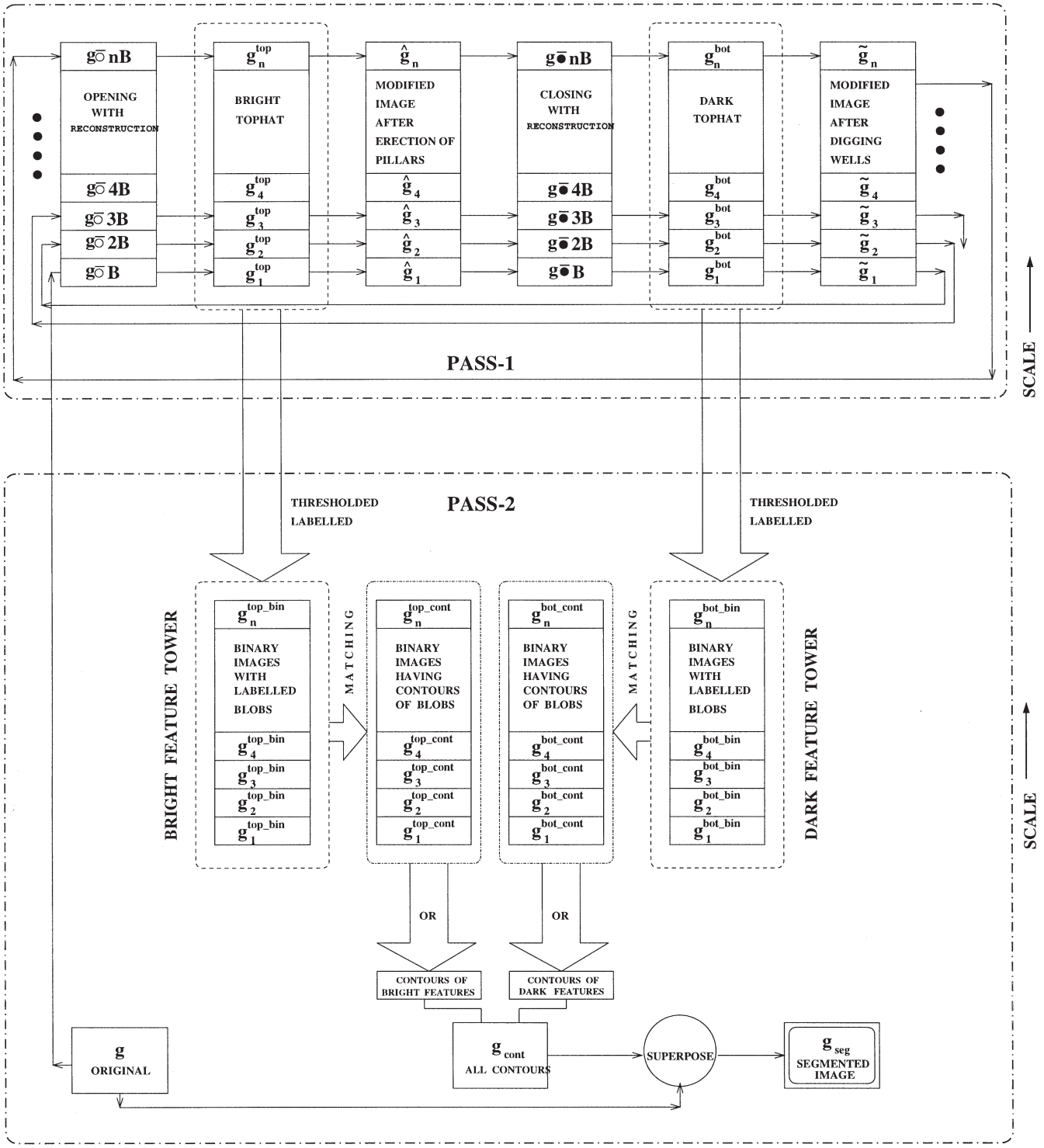

Fig. 6. Schematic diagram for multiscale image segmentation using morphological towers.

Similar approach may be found in [13]. The main problem of this approach is to determine the size of SE. Based on the domain knowledge and sensor parameters (namely, resolution and magnification factor) minimum size of the features of interest in the image can be determined in terms of pixels. Any feature of size smaller than that may be treated as noise. Size of isotropic SE to eliminate such noise can then simply be computed.

2) Pass-1: Multiscale Region Extraction: The preprocessed image works as the input to the first pass of our segmentation algorithm. In this pass the information about potential bright and dark regions at different scales are extracted by executing an alternate sequence of opening and closing (see Fig. 6). The bright top-hat image resulting due to opening at scale i is thresholded at level 0. The resulting binary image contains

all possible bright features in the image. However, all these features are not visually discernible. Only those features that have sufficient contrast with respect to its immediate background can readily be identified. Suppose Π_i^j is a component in the resultant binary image. Then local contrast is measured as

$$LC(\Pi_i^j) = [\max\{g(x, y) \,|\, (x, y) \in \Pi_i^j\}] - [\min\{g(x, y) \,|\, (x, y) \in \Pi_i^j\}]. \quad (30)$$

If the contrast is less than some specified threshold k, the corresponding component is discarded. Finally, the resultant binary image is kept in the ith level of the *bright_feature_tower*. It is then used as a mask for spatial locations of the input image where pillars of infinite altitude require to be erected according to equation (28). Then closing with an SE of scale i is performed on modified input image. Proceeding in the similar way as described in case of opening, another binary image is obtained which is kept in the ith level of the *dark_feature_tower*. This binary image is used to dig wells of infinite depth according to equation (29). However, in practice, the height of pillars and depth of wells are chosen as 255 and 0 respectively for 8-bit image. The erection of pillars and excavation of wells are performed using

$$g(x, y) = \begin{cases} MAXVAL, & \text{if } (x, y) \in \Pi_i \text{ and } LC(\Pi_i^j) \geq k \\ g(x, y), & \text{otherwise} \end{cases}$$

and

$$g(x, y) = \begin{cases} MINVAL, & \text{if } (x, y) \in \Upsilon_i \text{ and } LC(\Upsilon_i^j) \geq k \\ g(x, y), & \text{otherwise} \end{cases}$$

where $MINVAL = 0$ and $MAXVAL = 255$ and k is a threshold value.

At a glance, the steps in the multiscale region extraction are as given below. The following steps are performed starting with the preprocessed image as input.

1) The image is opened with a disk SE B. The bright top-hat image obtained by subtracting the opened image from the input image is then thresholded at the level 0. Components that do not have sufficient local contrast are then discarded. The resulting binary image $g_i^{top\_bin}$ consists of black blobs corresponding to visually discernible bright features. It is then stored in the ith level in the *bright_feature_tower*.
2) The binary image $g_i^{top\_bin}$ is then used as a mask for erecting pillars in the input image to prevent encroachment. The gray value of each pixel in the input image masked by this binary image is changed to 255.
3) The modified input image is closed with the same SE B. The dark top-hat image is subjected to the same operations as in case of bright top-hat image in step 1). As before, the resulting binary image $g_i^{bot\_bin}$ is saved in the ith level in the *dark_feature_tower*.
4) The binary image $g_i^{bot\_bin}$ is then used as a mask for digging wells in the input image to prevent encroachment. The gray value of each pixel in the input image masked by this binary image is changed to 0.
5) Select the next higher homothetic of the SE B and if it is not larger than that at the prescribed largest scale, go to step 1). Otherwise halt.

3) Pass-2: Selection of Valid Regions That Contribute to Final Segments: After building the towers in the first pass the second pass selects the valid segments at various scales that contribute to the final segmentation. By the term "valid segments" we mean either a self-contained complete object or a well-defined part of an object. The former is indicated by saturation, while the latter by merging. The closed contours of such regions are traced out and combined together to obtain the final result. Thus, in the second pass the valid bright segments are searched using the binary images kept in *bright_feature_tower*. We start with the image pair at the lower-most levels in the *bright_feature_tower*, set $i = 1$ and g_{bright_cont} to *null image*. Then the steps are:

1) Consider the ith and $(i + 1)$th binary images in the *bright_feature_tower*. Label the components of the images [3].
2) Modify $g_i^{top\_bin}$ by deleting all components except those which i) are identical in both $g_i^{top\_bin}$ and $g_{i+1}^{top\_bin}$ and ii) merge into a single component of $g_{i+1}^{top\_bin}$.
3) Trace the contours of the objects in binary image $g_i^{top\_bin}$. Let $g_i^{top\_cont}$ be the corresponding contour image.
4) Take the cumulative set-theoretic union of the images g_{bright_cont} and $g_i^{top\_cont}$.
5) Increase i. If $(i+1)$ is greater than the height of the tower, halt. Else go to step 1).

The image g_{bright_cont} contains the closed contours of all prominent bright segments in the input image.

We perform similar set of operations [i.e., steps 1)–5)] with all successive pairs of binary images in the *dark_feature_tower* and construct a contour image g_{dark_cont}. Finally, the image g_{cont} is obtained by combining g_{bright_cont} and g_{dark_cont}. The image g_{cont}, therefore, contains the closed contours of all bright and dark segments present in the image and is the result of the proposed scheme.

IV. Experimental Results and Discussions

The proposed algorithm has been executed on a set of images. Figs. 7(a)–10(a) show some of the test images used in the experiment. The images in Figs. 7(a) and 8(a) are synthetic images depicting dark and bright spheres of different radii. The image in Fig. 8(a) is generated by corrupting the image in Fig. 7(a) with random noise. Figs. 9(a) and 10(a) represent real images of blood cells and skin lesions respectively. The results produced by the proposed multiscale morphological segmentation algorithm are shown in Figs. 7(b)–10(b). The results have been compared with those of two other well known methods. The results of watershed segmentation algorithm are shown in Figs. 7(c)–10(c) in the identical order. The gradient images used in the watershed algorithms are obtained using morphological operations—more specifically it is the difference between the dilated and eroded versions of the image. The markers are the local minima of the gradient image which are obtained by comparing the original image and its eroded

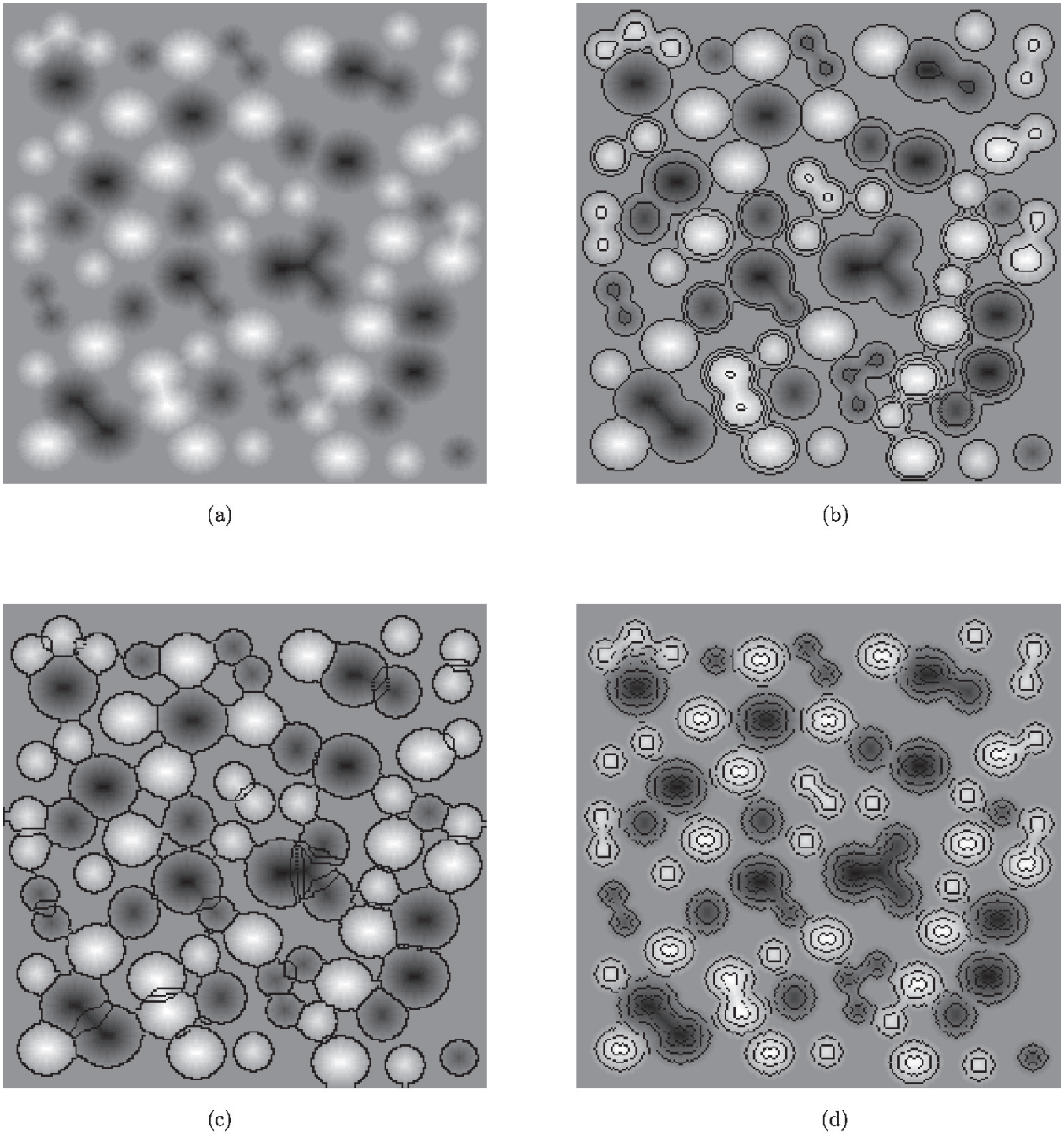

Fig. 7. Results of segmentation (a) (synthetic input) image of bright and dark balls of varying radii (b)–(d) output images, (b) multiscale morphological segmentation, (c) watershed segmentation, and (d) Canny's edge-based technique.

version. Figs. 7(d)–10(d) show the respective results of Canny's edge based segmentation technique. Contours obtained due to different methods are superposed on the respective original images for visual evaluation of the methods. Table I shows the values of different parameters used in the experiment in order to produce visually optimum results in each case. The minimum and the maximum value of the diameter of the SE is determined be the range of the size of the objects we are interested in. In all cases we have taken 7 as minimum diameter of SE. Contrast threshold k specifies how distinct the segment could be relative to its immediate background. It is important to observe the results in a greater detail to compare the performance. For subjective evaluation of performance of the said methods we concentrate on the following qualities of the segmentation results and judge them visually.

a) *Continuity:* The contours in case of all the images resulting due to the proposed method are closed and continuous [see Figs. 7(b)–10(b)]. The contours produced by

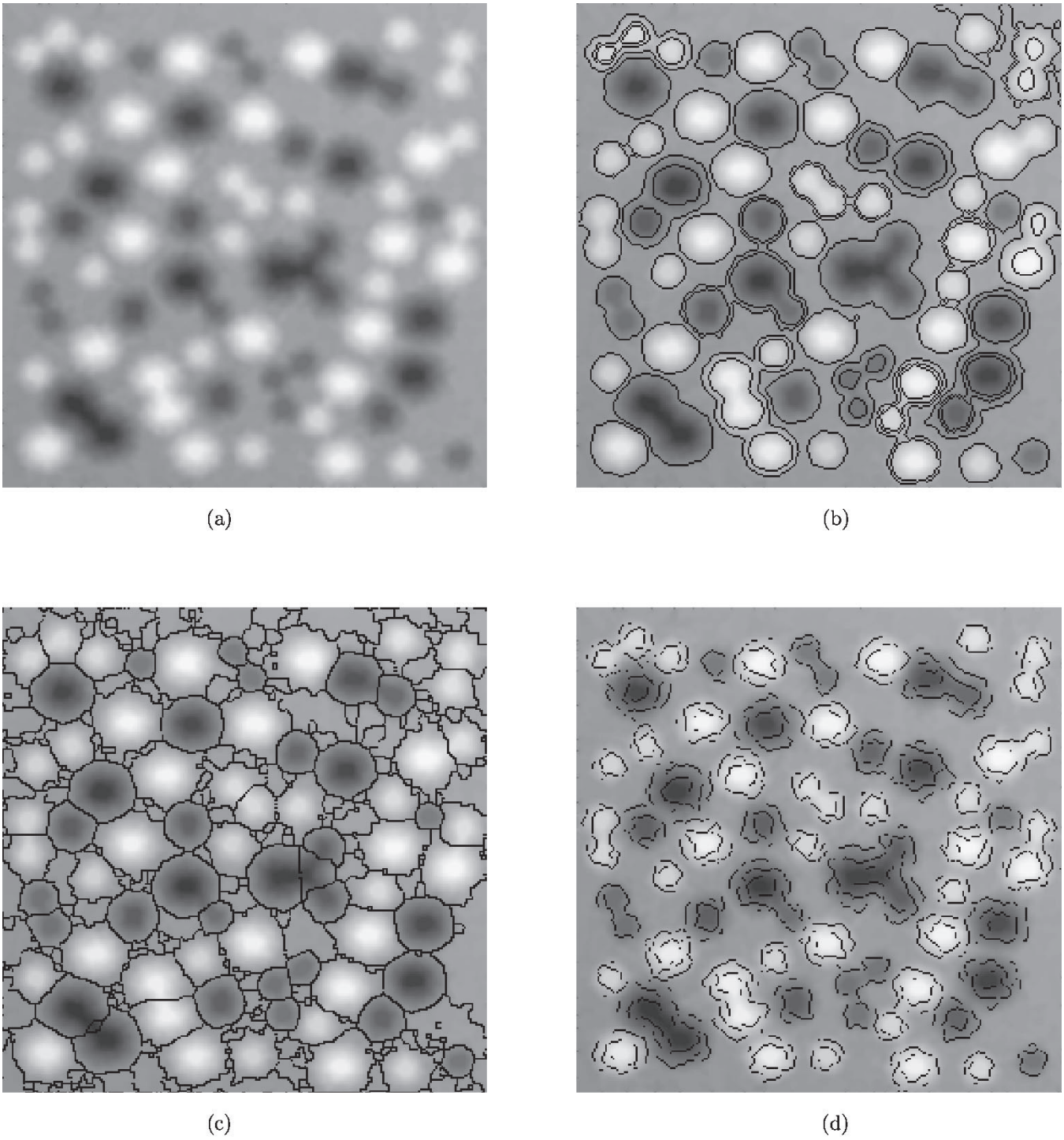

Fig. 8. Results of segmentation (a) (input image) noise-corrupted version of the image in Fig. 7(a) (b)–(d) output images, (b) multiscale morphological segmentation, (c) watershed segmentation, and (d) Canny's edge-based technique.

the watershed algorithm are not always continuous and closed as can be seen in Figs. 8(c)–10(c). The contours produced by Canny's edge based technique in all the resulting images are mostly discontinuous. Canny's edge also suffers from localization problem.

b) *Mutual exclusion:* The significant regions are successfully separated by contours produced by the proposed method. There is no encroachment among different adjacent segments in the output images produced by the proposed method. Mutual exclusion in regions are also observed in the results of watershed algorithm. However, no such comments made in case of Canny's method due to presence of open contours.

c) *Over- and under-segmentation:* The results of the proposed algorithm suffer from over-segmentation problem relatively less as compared to that of the watershed algorithm. Second, the problem of over-segmentation may further be reduced by increasing the size of the SE. The

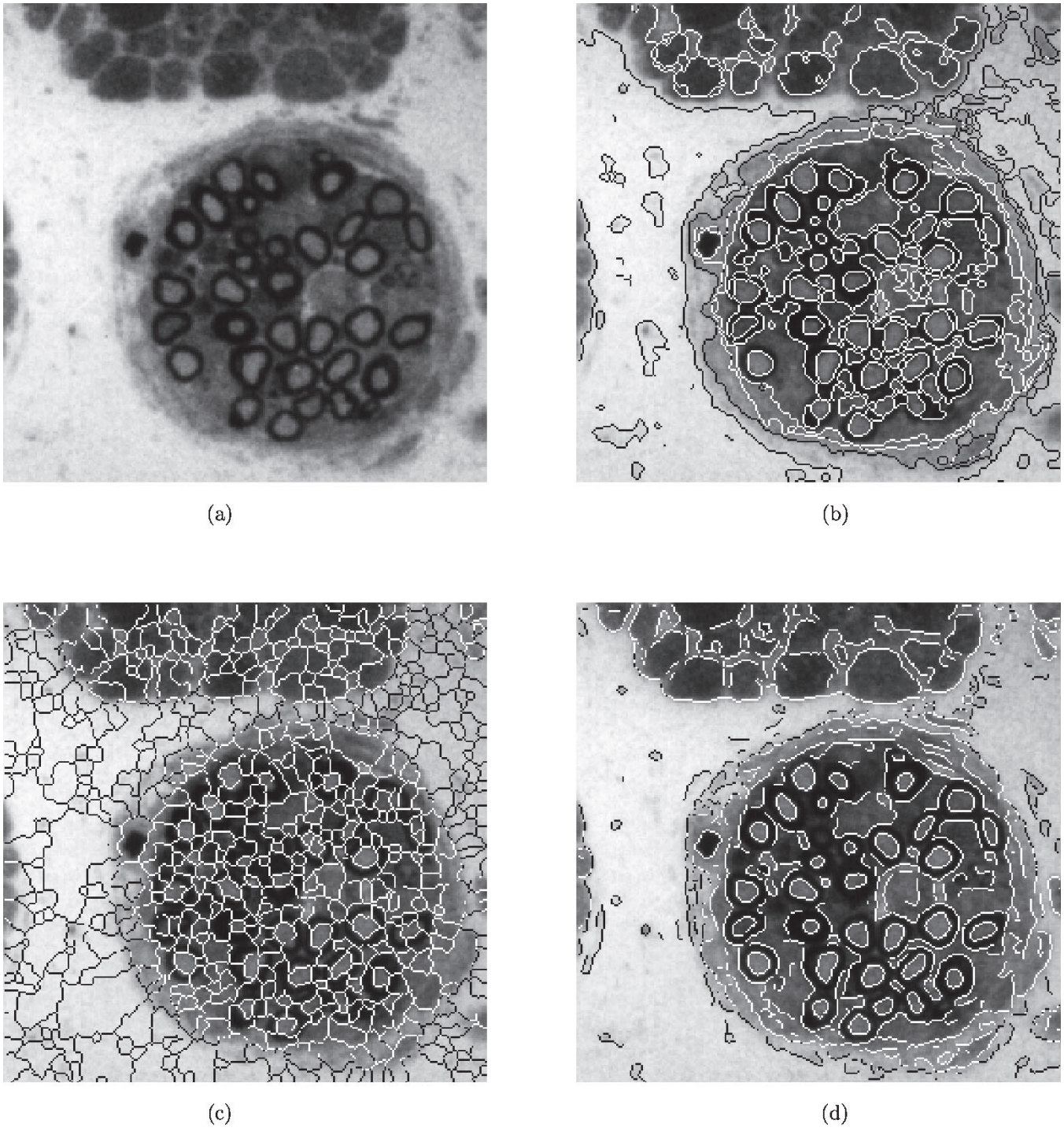

Fig. 9. Results of segmentation (a) (input) image of myelin, (b)–(d) output images, (b) multiscale morphological segmentation, (c) watershed segmentation, and (d) Canny's edge-based technique.

problem of over-segmentation is grossly present in case of watershed algorithm [see Figs. 8(c)–10(c)]. Canny's method, has however, produced under-segmented and improperly segmented output images.

d) *Emphasis on sub-features:* The proposed method has the option to emphasize on different sub-features of relatively large features. This is achieved due to *merging* and *saturation* criteria. We, however, have the option for suppressing the sub-features if we do not take the merging criterion into account. The concentric multiple contours appear if a feature continues to grow after attaining saturation criterion for some scale (see Fig. 3 and relevant text). The small sub-regions within relatively larger regions can be contoured separately. This cannot be done by other methods.

e) *Emphasis on shape and scale:* Emphasis on both shape and scale has been given in case of the proposed method. Emphasis on scale only is given in the case of Canny's

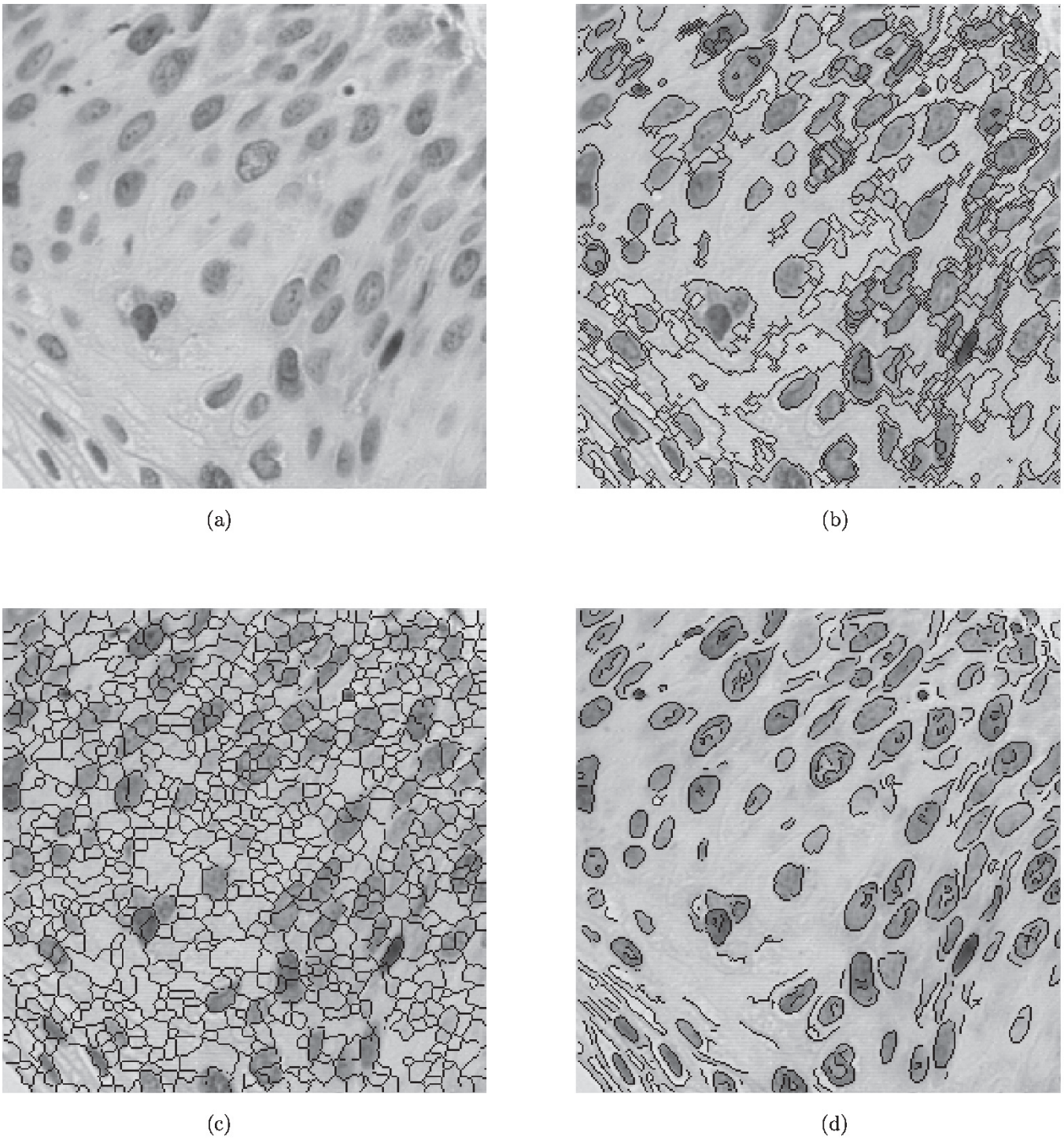

Fig. 10. Results of segmentation (a) (input) image of skin lesions (b)–(d) output images, (b) multiscale morphological segmentation, (c) watershed segmentation, and (d) Canny's edge-based technique.

edge based technique. No emphasis on shape and scale is given in the watershed algorithm.

f) *Other overheads:* The proposed algorithm makes use of two control parameters *viz.* the graylevel threshold k applied on the residual image and diameter of SE. The second parameter incorporates domain knowledge in terms of size of objects of interest. However, the results are not very sensitive to value of the threshold (k). The space-time complexity is very high and is mainly caused by the multiscale opening and closing by reconstruction. In each scale these operations involve computations of the order of mN^2, for an image of size $N \times N$, and m is a multiplier that depends on the scale factor. The time complexity may be improved significantly by distributing the operations at different scales on parallel processors. In case of watershed algorithm the selection of initial marker points is a crucial overhead on which the result depends heavily. The time complexity is also high. In

TABLE I
VALUES OF THE PARAMETERS USED IN THE EXPERIMENT

Serial No.	Fig. No.	Description of Image	MMS		CEST	
			Contrast threshold (k)	maximum diameter of SE	sigma	hysteresis
1	7(a)	bright and dark balls of different radii	5	43	0.742	35
2	8(a)	noisy 7(a)	5	51	0.750	30
3	9(a)	myelin	10	39	1.200	32
4	10(a)	skin lesions	11	59	1.000	40

MMS: Multiscale Morphological Segmentation, CEST: Canny's Edge based Segmentation Technique

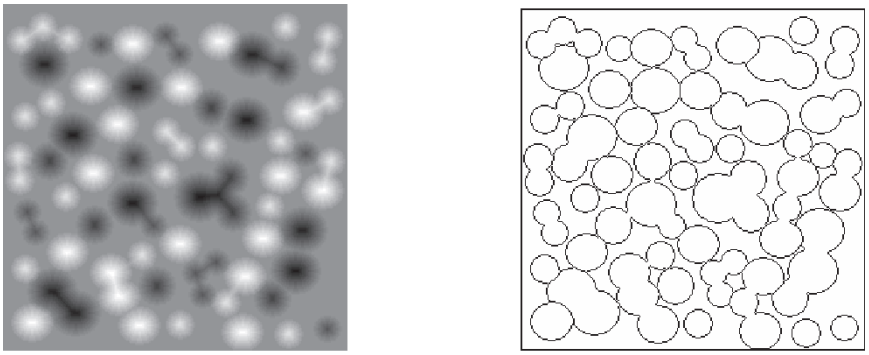

(a) (b)

Fig. 11. (a) The input image and (b) the ideal contour.

case of Canny's edge based technique two parameters, namely the scale and the hysteresis, have strong influence on the output. The space complexity is not as high as that of other two methods.

Here, we would like to mention the basic difference between the proposed method and the watershed algorithm as they are conceptually most similar. Both the algorithms adopt region-based approach. However, they perform the task in two different ways. The major differences are mentioned below.

The surface topography of a gray-scale image consists of hills and pits of various base sizes and heights or depths. In watershed algorithm the surface of the gradient image is submerged in an infinite source of water. Water enters through fictitious holes at different local minima of the gradient image and fills the catchment with a constant vertical upward speed. The waterline separating two or more such filled catchment basins constitute the segmentation contours of the image. Defining gradient image (by means of differentiation in discrete domain) and local minima of the catchment basins are two major sources of problems that results in over- and under-segmentation.

The proposed algorithm fills the troughs and truncates the peaks with a structuring element (SE) whose scale increases at a constant rates. So, there is no need of searching for the local minima or maxima. The starting scale of the SE automatically takes care of this. It is not necessary to fill the troughs or truncate the peaks at constant speed or rate. It avoids to work on the gradient image. The proposed algorithm takes care of both bright and dark segments in the same pass without allowing any mutual encroachment. The contours are generated from information extracted at different scales subject to three prescribed criteria, namely growing, saturation and merging. So the segments extracted are scale-calibrated and shape preserving.

The initialization, implementation of watershed algorithm is relatively more complicated as compared to those of the proposed method. Secondly, Watershed algorithm might give rise to broken waterlines and, hence, broken contours in some cases as it works on gradient image. The proposed algorithm is guaranteed to give closed contours. It may also mark and extract well defined sub-regions. However, the space-time complexity of the proposed method is relatively higher on sequential machines. So it may be recommended for parallel machines.

A. Performance Analysis

For quantitative analysis of the performance of the segmentation algorithms used in this work, we propose a simple measure based on similarity between the contours generated by the respective algorithms with the ideal ones. The synthetic image shown in Fig. 7(a) consisting of bright and dark spheres of different radii is chosen as a reference image for performance analysis [and it is redisplayed in Fig. 11(a)]. The ideal contours segmentation are shown in Fig. 11(b). The contours produced by a segmentation algorithm must be very close or similar to the ideal ones.

TABLE II
RELATIVE PERFORMANCE OF THE SEGMENTATION ALGORITHMS

Correct Segmentation Factor CSF			
$MMS-I$	WSD	$CEST$	$MMS-II$
1.6957	1.4645	2.6019	0.1280

MMS-I: Multiscale Morphological Segmentation, WSD: Watershed algorithm, CEST: Canny's Edge based Segmentation Technique, MMS-II: Multiscale Morphological Segmentation with no emphasis on sub-features.

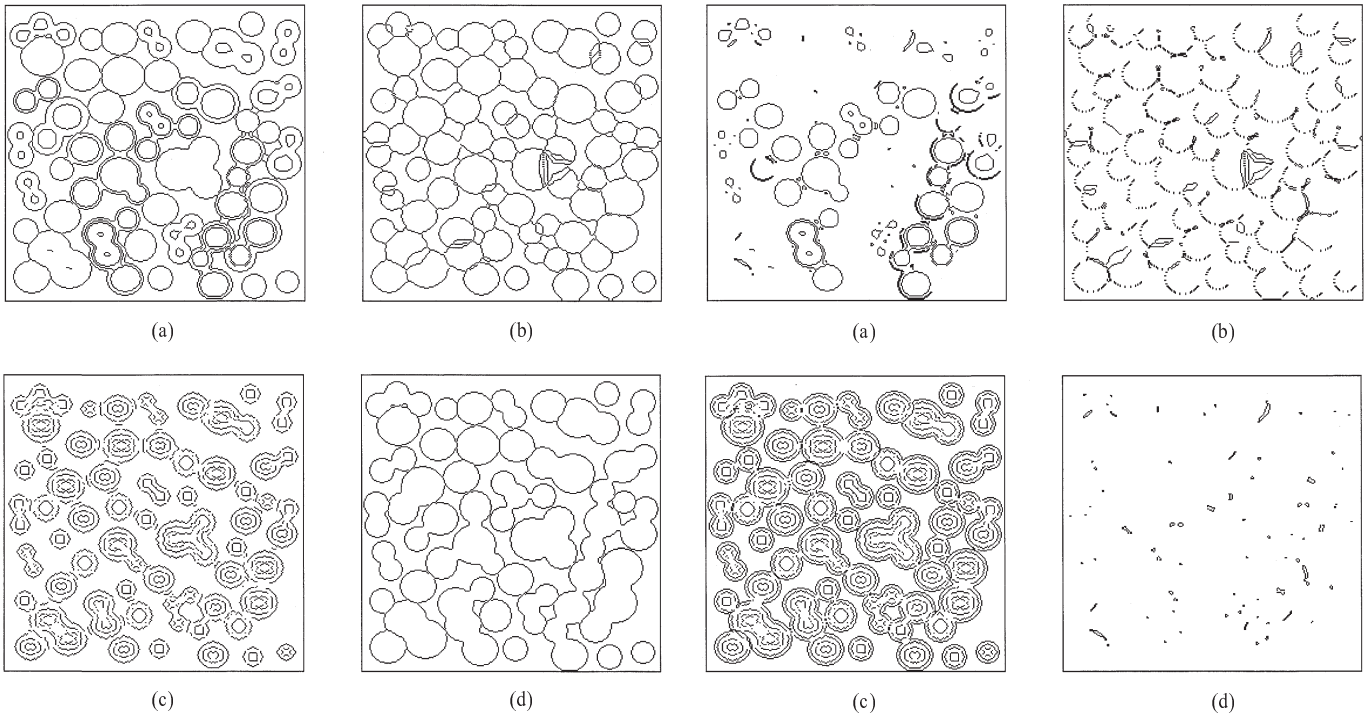

Fig. 12. Segmentation contours traced by (a) multiscale morphological segmentation, (b) watershed segmentation, (c) Canny's edge-based segmentation and (d) multiscale morphological segmentation with no emphasis on sub-features.

Fig. 13. Images generated by pixel-wise exclusive-OR operation between the ideally segmented image and the image generated (a) multiscale morphological segmentation, (b) watershed segmentation, (c) Canny's edge-based segmentation and (d) multiscale morphological segmentation with no emphasis on sub-features.

Let I_{id} and I_{sg} be the binary images which consist of ideal and extracted contours respectively. The pixel-wise *exclusive-OR* operation (31) between them gives an idea of mismatch

$$I_{op}[x][y] = I_{id}[x][y] \tilde{\oplus} I_{sg}[x][y] \tag{31}$$

where $\tilde{\oplus}$ denotes the exclusive-OR operation.

If N_{id} and N_{op} be total number of black pixels in the images I_{id} and I_{op} respectively, we define the *correct segmentation factor* CSF as

$$CSF = \frac{N_{op}}{N_{id}}. \tag{32}$$

For an ideal segmentation the value of CSF should be zero. However, smaller value of CSF indicates better performance. Table II shows the values of CSF for three algorithms executed on the image of Fig. 11(a). Fig. 12(a)–(c) show the contours produced by the proposed method, Watershed algorithm and Canny's edge based technique. The results of pixel-wise *exclusive-OR* operation are shown in Fig. 13(a)–(c).

The high value of CSF in case of the proposed method is mainly contributed by the contours of sub-features. However, without using the merging criteria and adjusting the scale-parameter, we can avoid extracting the sub-features [see Fig. 12(d)]. As a result there is a significant reduction in CSF as shown in Table II. In watershed algorithm a pixel equidistant from two adjacent catchment basins require an arbitration as it may simultaneously be claimed by both of them. The arbitration may cause a drift in waterlines. As a result the CSF increases. Canny's algorithm employs convolution of image with Gaussian function. As a result the contours are drifted from the ideal position which along with discontinuity results in high value of CSF.

V. CONCLUSION

In this paper, we have proposed a scheme for segmenting gray-level images of cluttered objects of different shape and

size. The proposed multiscale morphological method is expected to work satisfactorily on gray-level images containing bright and dark features of various scales. The scheme starts with simplifying the image in the preprocessing step. In the first pass the algorithm extracts potential regions at various scales by multiscale top- and bottom-hat transformation and store them in different towers. In the second pass the algorithm compares pair of feature images corresponding to two successive scales and identifies the potential regions that contribute to final segmentation based on three criteria, namely *growing*, *merging*, and *saturation*. Finally the contours of all such potential regions are integrated. The results of the proposed scheme have been compared with those of two other well known methods, namely watershed algorithm and Canny's edge-based algorithm. It is evident that the results produced by Canny's method are far behind than those of the proposed scheme and watershed algorithm for the class of images we consider. The watershed algorithm produce over-segmentation in some cases. The proposed method, by and large, produce overall better results compared to two other methods. The positive features of the proposed scheme is that it is *shape*- and *edge-preserving*, *scale-calibrated*, and satisfy a set of goodness criteria. However, the CPU time and memory space requirement of the scheme are relatively higher. The proposed scheme being inherently parallel might improve this shortcoming after suitable parallel implementation.

REFERENCES

[1] A. K. Jain, *Fundamentals of Digital Image Processing*. Englewood Cliffs, NJ: Prentice-Hall, 1989.

[2] K. S. Fu, "A survey on image segmentation," *Pattern Recognit.*, vol. 13, pp. 3–16, 1981.

[3] A. Rosenfeld and A. C. Kak, *Digital Picture Processing*, 2nd ed. New York: AP, 1982, vol. 1/2.

[4] B. Chanda and D. Dutta Majumder, *Digital Image Processing and Analysis*. New Delhi: Prentice-Hall of India, 2000.

[5] ——, "A note on use of gray-level co-occurrence matrix in threshold selection," *Signal Process.*, vol. 15, no. 2, pp. 149–167, 1988.

[6] B. Chanda, B. B. Chaudhuri, and D. Dutta Majumder, "A modified scheme for segmenting noisy images," *IEEE Trans. Syst., Man, Cybern.*, vol. 18, no. 3, pp. 458–467, 1988.

[7] J. S. Weszka and A. Rosenfeld, "Threshold evaluation techniques," *IEEE Trans. Syst., Man, Cybern.*, vol. SMC-8, pp. 622–629, 1978.

[8] J. F. Canny, "A computational approach to edge detection," in *Readings in Computer Vision: Issues, Problems, Principles and Paradigms*, M. A. Fischler and O. Firschein, Eds. San Mateo, CA: Morgan Kaufmann, 1986, pp. 184–203.

[9] B. M. ter Haar Romeny, Ed., *Geometry-Driven Diffusion in Computer Vision*. Dordrecht, The Netherlands: Kluwer, 1994.

[10] J. Weickert, *Anisotropic Diffusion in Image Processing*, ser. ECMI. Stuttgart, Germany: Teubner-Verlag, 1998.

[11] W. J. Niessen, K. L. Vincken, J. Weickert, and M. A. Viergever, "Nonlinear multiscale representations for image segmentation," *Comput. Vis. Image Understand.*, vol. 66, pp. 233–245, 1997.

[12] P. T. Jackway, "Gradient watershed in morphological scale-space," *IEEE Trans. Image Processing*, vol. 5, pp. 913–921, 1996.

[13] J. H. Bosworth and S. T. Acton, "Morphological image segmentation by local monotonicity," in *Proc. Asilomar Conf. Signals, Systems, and Computers*, vol. 1, Pacific Grove, CA, Oct. 24–27, 1999, pp. 53–57.

[14] R. J. Frank, T. J. Grabowski, and H. Damasio, "Voxelvise percentage tissue segmentation of human brain magnetic resonance images (abstract)," in *Abstracts, 25th Annual Meeting, Society for Neuro-Science*. Washington, DC: Society for Neuro-science, 1995, p. 694.

[15] V. D. Heijden, "Edge and line feature extraction based on covariance models," *IEEE Trans. Pattern Anal. Machine Intell.*, vol. 17, pp. 69–77, 1995.

[16] J. Gauch and C. W. Hsia, "A comparison of three color image segmentation algorithms in four color spaces," *Proc. SPIE*, vol. 1818, pp. 1168–1181, 1992.

[17] R. Schettini, "A segmentation algorithm for color images," *Pattern Recognit. Lett.*, vol. 14, pp. 499–506, 1993.

[18] T. Vlachos and A. G. Constantinides, "Graph-theoretical approach to color picture segmentation and contour classification," *Proc. Inst. Elect. Eng.*, vol. 140, pp. 36–45, 1993.

[19] M. Goldberg and J. Zhang, "Hierarchical segmentation using a composite criterion for remotely sensed imagery," *Photogrammetria*, vol. 42, pp. 87–96, 1987.

[20] H. Digabel and C. Lantuejoul, "Iterative algorithms," in *Proceedings of the 2nd European Symposium Quantitative Analysis of Microstructures in Material Science, Biology and Medicine*. Stuttgart, Germany: Riederer Verlag, 1977, 1978, pp. 85–99.

[21] S. Beucher, "Watersheds of functions and picture segmentation," in *Proc. IEEE Int. Conf. Acoustics, Speech, and Signal Processing*, Paris, France, 1982, pp. 1928–1931.

[22] F. Meyer and S. Beucher, "Morphological segmentation," *J. Vis. Commun. Image Represent.*, vol. 1, pp. 21–46, 1990.

[23] J. Shi and J. Malik, "Normalized cuts and image segmentation," *IEEE Trans. Pattern Anal. Machine Intell.*, vol. 22, pp. 888–905, Aug. 2000.

[24] W. Y. Ma and B. S. Manjunath, "EdgeFlow: A technique for boundary detection and segmentation," *IEEE Trans. Image Processing*, vol. 9, pp. 1975–1988, Aug. 2000.

[25] J. Z. Wang, J. Li, R. M. Gray, and G. Wiederhold, "Unsupervised multiresolution segmentation for images with low depth of field," *IEEE Trans. Pattern Anal. Machine Intell.*, vol. 23, no. 1, pp. 85–90, 2001.

[26] H. Atmaca, M. Bulut, and D. Demir, "Histogram based fuzzy Kohonen clustering network for image segmentation," in *Proc. Int. Conf. Image Processing*, 1996, p. 18A6.

[27] J. K. Udupa and S. Samarasekera, "Fuzzy connectedness and object definition: Theory, algorithms, and applications in image segmentation," *Graph. Mod. Image Process.*, vol. 58, pp. 246–261, 1996.

[28] D. N. Chun and H. S. Yang, "Robust image segmentation using genetic algorithm with a fuzzy measure," *Pattern Recognit.*, vol. 29, pp. 1195–1211, 1996.

[29] A. Betti, M. Barni, and A. Mecocci, "Using a wavelet-based fractal feature to improve texture discrimination on SAR images," in *Proc. 1997 Int. Conf. Image Processing (ICIP '97)*, vol. 1, Washington, DC, Oct. 26–29, 1997.

[30] R. Acharya and R. P. Menon, "A review of biomedical image segmentation techniques," in *Deformable Models in Medical Image Analysis*, A. Singh, D. Goldgof, and D. Terzopoulos, Eds. Los Alamitos, CA: IEEE Computer Soc., 1998, pp. 140–161.

[31] G. M. Matheron, *Random Sets and Integral in Geometry*. New York: Wiley, 1975.

[32] J. Serra, *Image Analysis Using Mathematical Morphology*. London, U.K.: Academic, 1982.

[33] P. Salembier and J. Serra, "Morphological multiscale image segmentation," in *Proc. Visual Communication and Image Processing*, Boston, MA, 1992, pp. 620–631.

[34] P. Salembier, "Morphological multiscale segmentation for image coding," *Signal Process.*, vol. 38, pp. 359–386, 1994.

[35] P. T. Jackway, "Multiscale image processing: A review and some recent developments," *J. Elect. Electron. Eng. Australia*, vol. 13, no. 2, pp. 88–98, 1993.

[36] A. Rosenfeld and A. C. Kak, *Digital Picture Processing*, 2nd ed. New York: Academic, 1982, vol. 1/2.

[37] R. V. D. Boomgaard and L. Dorst, "The morphological equivalent of Gaussian scale-space," in *Gaussian Scale-Space Theory*, J. Sporring, M. Nielsen, L. Florack, and P. Johansen, Eds. Amsterdam, The Netherlands: Kluwer, 1997, vol. 8.

[38] A. P. Witkin, "Scale-space filtering: A new approach to multiscale description," in *Image Understanding*, S. Ullman and W. Richards, Eds. Norwood, NJ: Ablex, 1984, pp. 79–95.

[39] P. T. Jackway and M. Deriche, "Scale-space properties of multiscale dilation-erosion," *IEEE Trans. Pattern Anal. Machine Intell.*, vol. 18, pp. 38–51, 1996.

[40] P. T. Jackway, "Morphological scale-space," in *Proc. 11th IAPR Int. Conf. Pattern Recognition*, The Hague, The Netherlands, September 1992, pp. 252–255. P. Salembier, "Morphological multiscale segmentation for image coding," *Signal Process.*, vol. 38, pp. 359–386, 1994.

[41] R. M. Haralick and L. G. Shapiro, *Computer and Robot Vision*. Reading, MA: Addison-Wesley, 1992, vol. 1.
[42] P. Maragos, "Pattern spectrum and multiscale shape representation," *IEEE Trans. Pattern Anal. Machine Intell.*, vol. 11, pp. 701–716, 1989.
[43] A. Toet, "A hierarchical morphological image decomposition," *Pattern Recognit. Lett.*, vol. 11, no. 4, pp. 267–274, Apr. 1990.
[44] L. M. Lifshitz and S. M. Pizer, "Multi-resolution hierarchical approach to image segmentation based on intensity extrema," *IEEE Trans. Pattern Anal. Machine Intell.*, vol. 12, pp. 529–540, June 1990.
[45] P. Perona and J. Malik, "Scale-space and edge detection using anisotropic diffusion," *IEEE Trans. Pattern Anal. Machine Intell.*, vol. 12, pp. 629–639, July 1990.
[46] J. A. Bangham, R. Harvey, P. D. Ling, and R. V. Aldridge, "Morphological scale-space preserving transforms in many dimensions," *J. Electron. Imag.*, vol. 5, no. 3, pp. 283–299, July 1996.
[47] P. Salembier and M. Pardas, "Hierarchical morphological segmentation for image sequence coding," *IEEE Trans. Image Processing*, vol. 3, pp. 639–651, Sept. 1994.
[48] C. Lantuejoul and F. Maisonneuve, "Geodesics methods in image analysis," *Pattern Recognit.*, vol. 17, pp. 117–187, 1984.
[49] P. Salembier and J. Serra, "Flat zones filtering, connected operators and filters by reconstruction," *IEEE Trans. Image Processing*, vol. 4, no. 8, pp. 1153–1160, 1995.
[50] S. Mukhopadhyay and B. Chanda, "Fusion of 2D gray-scale images using multiscale morphology," *Pattern Recognit.*, vol. 34, no. 10, pp. 1939–1949, Oct. 2001.
[51] ——, "A multiscale morphological approach to local contrast enhancement," *Signal Process.*, vol. 80, pp. 685–696, 2000.
[52] ——, "An edge preserving noise smoothing technique using multiscale morphology," *Signal Process.*, vol. 82, no. 4, pp. 527–544, 2002.
[53] D. C. Marr and E. Hildreth, "Theory of edge detection," in *Proc. R. Soc. Lond.*, vol. B, 1962, pp. 187–217.

Susanta Mukhopadhyay received his B.Sc.(Hons) in physics from Presidency College, Calcutta, India, in 1988, and the B.Tech. and M.Tech. degrees in radiophysics and electronics from University of Calcutta in 1992 and 1994, respectively. He received the Ph.D. degree in 2003 from Indian Statistical Institute, Calcutta. His Ph.D. work was related to multiscale image processing under the framework of mathematical morphology.

He has been working as a Research Associate at the Burnham Institute, La Jolla, CA, since 2001.

Bhabatosh Chanda (S'82–M'85–F'03) was born in 1957. He received the B.E. degree in electronics and telecommunication engineering and the Ph.D. degree in electrical engineering from the University of Calcutta, India, in 1979 and 1988, respectively.

He was with the Intelligent System Lab, University of Washington, Seattle, WA, as a Visiting Faculty from 1995 to 1996. He has published more than 70 technical articles. His research interest includes image processing, pattern recognition, computer vision, and mathematical morpholgy. He is currently a Professor at the Indian Statistical Institute, Calcutta.

Dr. Chanda received the "Young Scientist Medal" of the Indian National Science Academy in 1989, the "Computer Engineering Division Medal" of the Institution of Engineers (India) in 1998, and the "Vikram Sarabhai Research Award" of the Physical Research Lab. He is also recepient of a U.N. Fellowship, UNESCO-INRIA Fellowship, and Diamond Jubilee Fellowship of the National Academy of Sciences, India. He is a fellow of the National Academy of Sciences, India.